

# Broadband Array of Electromagnetic Induction Sensors for Detecting Buried Landmines

Waymond R. Scott, Jr.

School of Electrical and Computer Engineering  
Georgia Institute of Technology  
Atlanta, Georgia 30332-0250  
waymond.scott@ece.gatech.edu

**Abstract**— A broadband electromagnetic induction (EMI) sensor is developed to help discriminate between buried landmines and metal clutter. The detector uses a single dipole transmit coil and an array of three quadrupole receive coils. The sensor operates in the frequency domain and collects data at 21 logarithmically spaced frequencies from 300 Hz to 90 kHz. Experimental results are presented for several targets.

**Keywords:** Electromagnetic Induction, EMI, Mine, Landmine, Metal Detector.

## I. INTRODUCTION

For many years, extensive effort has been expended developing techniques for efficiently locating buried landmines. For a mine detection technique to be successful, there must be sufficient contrast between the properties of the mine and the earth. There also must be sufficient contrast between the properties of the mine and common types of clutter such as rocks, roots, cans, etc. so that the mine can be distinguished from the clutter. The latter condition is the most problematic for most mine detection techniques. For example, simple electromagnetic induction (EMI) sensors are capable of detecting most mines; however, they will also detect every buried metal object such as bottle tops, nails, shrapnel, bullets, etc. This results in an unacceptable false alarm rate. This is even more problematic for low-metal anti-personnel mines as they are extremely difficult to distinguish from clutter using a simple EMI sensor. In recent years, advanced EMI sensors that use a broad range of frequencies or a broad range of measurement times along with advanced signal processing have been shown to be capable of discrimination between buried land mines and many types of buried metal clutter [1-4]. For these advanced EMI sensors to be effective, they must be able to accurately, repeatedly, and quickly measure the response of a buried target with a bandwidth greater than 100 to 1 while accurately measuring extremely weak signals.

The sensor developed for this work uses a single dipole transmit coil and an array of three quadrupole receive coils constructed using PCB technology, as in figure 1. A prototype system using this array is presented that operates over the frequency range 300 Hz to 90 kHz, a 300 to 1 bandwidth. This system evolved from an earlier system with a dipole receive

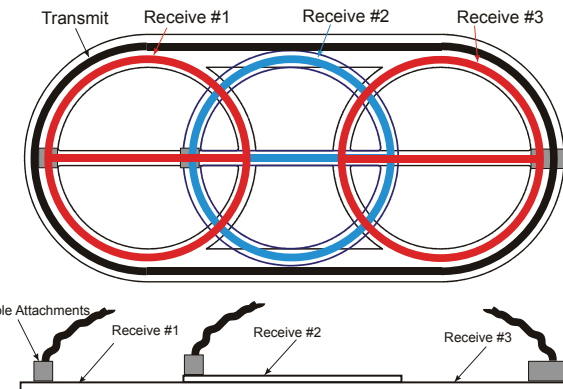


Figure 1. Diagram of the quadrupole array.

coil [5]. Sample measurements made with the system are shown.

## II. SYSTEM

Figure 2 shows a basic diagram of the system with a dipole transmit and a quadrupole receive coil that are used along with a secondary reference transformer. Here, the exciting current  $I_o$  passes through the primary coils of both the reference and head transformers and induces a voltage in the secondary of the transformers. The voltage induced in the secondary windings of the head transformer depends on its direct coupling as well

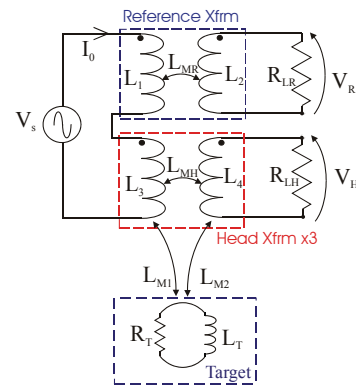


Figure 2. Schematic diagram of the system.

This work is supported in part by the U.S. Army Research Office under contract number W911NF-05-1-0257.

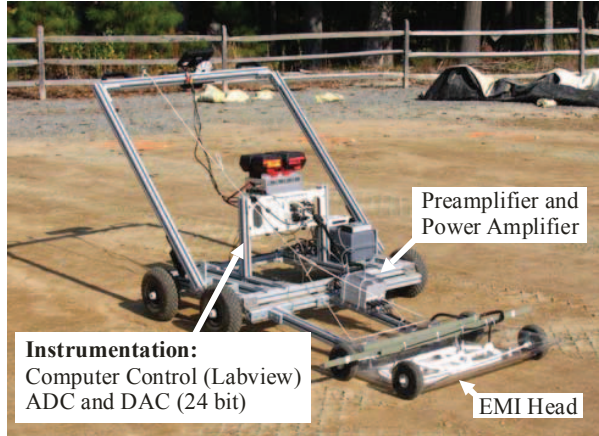


Figure 3. Cart-based EMI data collection system.

as the coupling through the target:

$$V_H = D(\omega) - \frac{\omega^2 L_{M1} L_{M2}}{R_T + j\omega L_T} I_0 .$$

Here  $D(\omega)$  represents the direct coupling between the coils of the head transformer and is due to both the inductive and capacitive coupling between the coils. The inductive and capacitive coupling between the transmit and receive coils is very small because of the manner in which the coils are wound. The voltage induced in the secondary coils of the reference transformer depends only on its mutual inductance:

$$V_R = -j\omega L_{MR} I_0 .$$

The response of the target is obtained from the relation

$$R = \frac{V_H - D(\omega)}{V_R} = \frac{j\omega L_{M1} L_{M2}}{L_{MR}(R_T + j\omega L_T)}$$

where  $D(\omega)/V_R$  is obtained by measuring a response without a target present.

The coupling between the coils of the EMI head and the target is not purely inductive as in the model, figure 2. Part of the coupling is due to the capacitance between coils and the target. The capacitive coupling can be comparable to or larger than the inductive coupling with the target. The capacitive coupling can vary significantly as an unshielded EMI head is moved in close proximity to the soil and can mask/corrupt the inductive responses of the desired targets. The effect is most problematic at the higher frequencies. Thus, a shield is needed to lessen the capacitive interactions. Ideally, the shield will completely eliminate the variations in the capacitive coupling due to the presence of the soil or other objects that are in close proximity to the head while not affecting the inductive coupling to the target. The shield developed for this work is similar to that developed earlier [5]. The shield is made using PCB technology and consists of closely spaced conducting rings with a gap so the rings will not form closed loops. The narrow width of the rings and the gap in the rings greatly reduce the eddy currents induced on the shield.

The data for the prototype system was taken at 21 frequencies that were approximately logarithmically spaced from 330 HZ to 90.03 KHz. The frequencies deviated from logarithmic spacing to minimize interference from power line harmonics. A multi-sine excitation signal was generated using the 21 frequencies and used to excite the EMI sensor. The response due to this multi-sine excitation was recorded in 0.1 s increments. These time records were transformed into the frequency domain and used to construct the response of the sensor.

### III. EXPERIMENTAL RESULTS

The prototype system was used to collect data at a test facility. The test facility consisted of a number of lanes divided into 1.5 by 1.5 m squares. A target was buried at the center of most of the squares. The data was collected in a lane based manner in which the sensor was pushed down the lane and the response was recorded in 0.1 s time increments along with the down-track location in the grid.

The measured data are filtered in the down-track direction by convolving the measured data with the zero-mean template shown in figure 4a. The magnitude of the response for all 21

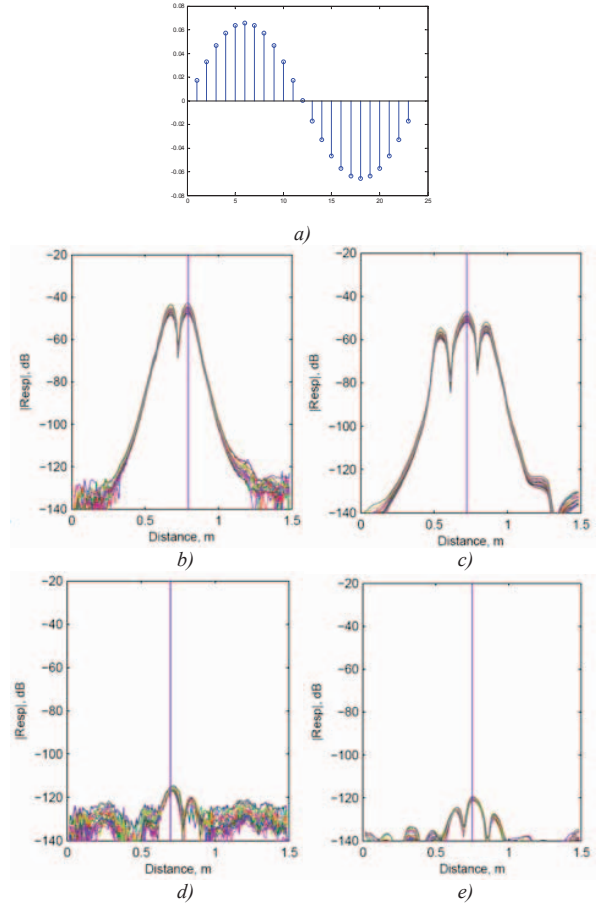


Figure 4. a) Down-track filter template. Down-track response for b) unfiltered and c) filtered PMD mine 0 cm deep. Down-track response for d) unfiltered and e) filtered M14 mine 5 cm

frequencies is shown in figure 4 as a function of down-track distance for a PMN and an M-14 landmine before and after filtering. The unfiltered response for both mines is weak directly above the mine and has a peak on either side of the mine due to the quadrupole receive coil. The filter has four beneficial effects. First, it mostly removes the ground response by differencing closely located portions of the ground. Second, it mostly removes the drift in the system by differencing measurements made only a short time apart. Third, it averages the data over several locations which will improve the signal to noise ratio. Fourth, the filtered data has a maximum directly over the target, while the unfiltered data has a minimum directly over the target. The filtered response of the M14 mine is much better defined than that of the unfiltered response. The noise floor is approximately -135 dB for the filtered response, which is about 10 dB better than for the unfiltered response. Note that the peak response for the M-14 mine is very weak, about -120 dB, while the response for the PMN mine is much stronger.

The response from multiple occurrences of four landmines is shown in figure 5 for all three receive channels when the landmine is approximately below the center receive head. The responses are graphed on Argand diagrams where the imaginary part of the response is graphed as a function of the real part with frequency as a parameter. The curves are shifted along the real axis so that they are centered; this further removes part of the ground response which is mostly a shift in the real part of the response. The fidelity of the data is generally apparent on this type of graph which makes it a good way to show the measured data. These graphs are very similar to the Cole-Cole graphs commonly used to show the complex permittivity of materials with dipolar type relaxations.

The shapes of the curves on the Argand diagrams are indicative of the type and distribution of metal in a target. The response of a simple target with a single relaxation will form a perfect semicircle on this type of graph. The response of each of the mines has a characteristic shape. The M-14 has a shape that is almost a semicircle indicating that its response is mostly due to a single relaxation. The other mines have more complex shapes indicating that their response is due to multiple relaxations. Note that the shapes of the curves for each mine are consistent in that they are scaled replicas of each other. The scaling of the response is due to the burial depth of the mine. The response is weaker for the deeper mines. Because these shapes of the different targets are quite different, it is possible to discriminate between some landmines and many types of clutter [6].

The response from the center channel is stronger than the side channels for all of the mines, as expected. The response is strongest in the channel closest to the mine. The response in the side channels is apparent on these graphs for a few of the mines when they are slightly off center. Note that the shape of the response in the side channels is almost the same as in the center channel. The response of the stronger mines would be readily apparent in a graph like figure 4 due to the higher dynamic range of the graph.

The responses at the center of the blank grid locations are graphed on Argand diagram in figure 6. Ideally these

responses will be zero; however, they are clearly nonzero and have a defined structure. The responses mostly take the shape of a line parallel to the real axis with a length proportional to their imaginary part. The real part is approximately proportional to  $\ln(f)$ . This response is believed to be due to the magnetic response of the soil which is not completely removed by the down-track filter since the magnetic properties of the soil vary with position. This response is very similar to that due to a magnetic material with a uniform logarithmic distribution of relaxation times [7-9].

#### IV. ACKNOWLEDGEMENT

The author would like to thank Dr. Gregg D. Larson for constructing the data collection system and helping with the field measurements.

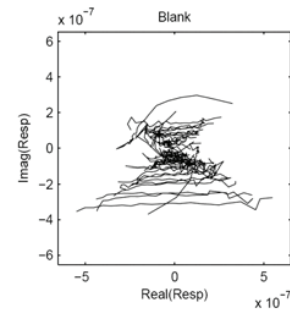


Figure 6. Respose plotted on an Argand diagram over the center of empty grid locations.

#### REFERENCES

- [1] P. Gao, L. Collins, P.M. Garber, N. Geng, and L. Carin, "Classification of Landmine-Like Metal Targets Using Wideband Electromagnetic Induction," *IEEE Transactions on Geoscience and Remote Sensing*, Vol. 38, No. 3, May 2000.
- [2] L. Collins, P. Gao, and L. Carin, "An Improved Bayesian Decision Theoretic Approach for Land Mine Detection," *IEEE Transactions on Geoscience and Remote Sensing*, Vol. 37, No. 2, March 1999.
- [3] G. D. Sower and S. P. Cave, "Detection and identification of mines from natural magnetic and electromagnetic resonances," in *Proc. SPIE*, Orlando, FL, 1995.
- [4] C. E. Baum, "Low Frequency Near-Field Magnetic Scattering from Highly, but Not Perfectly Conducting Bodies," Phillips Laboratory, Interaction Note 499, Nov. 1993.
- [5] Scott, W.R., Jr., "Broadband electromagnetic induction sensor for detecting buried landmines," *Proceedings of the 2007 IEEE Geoscience and Remote Sensing Symposium*, Barcelona, Spain, July 2007
- [6] E.B. Fails, P.A. Torrione, W. R. Scott, Jr, and L.M. Collins, "Performance of a four parameter model for modeling landmine signatures in frequency domain wideband electromagnetic induction detection systems," *Proceedings of the SPIE: 2007 Annual International Symposium on Aerospace/Defense Sensing, Simulation, and Controls*, Vol. 6553, Orlando, FL, May 2007.
- [7] S. Chikazumi, *Physics of Magnetism*, Wiley, New York, 1964.
- [8] Y. Das, "Effects of magnetic soil on metal detectors: preliminary experimental results," *Proc. SPIE* 6553, 655306 (2007)
- [9] Gordon F. West and Richard C. Bailey, "An instrument for measuring complex magnetic susceptibility of soils," *Proc. SPIE* 5794, 124 (2005)

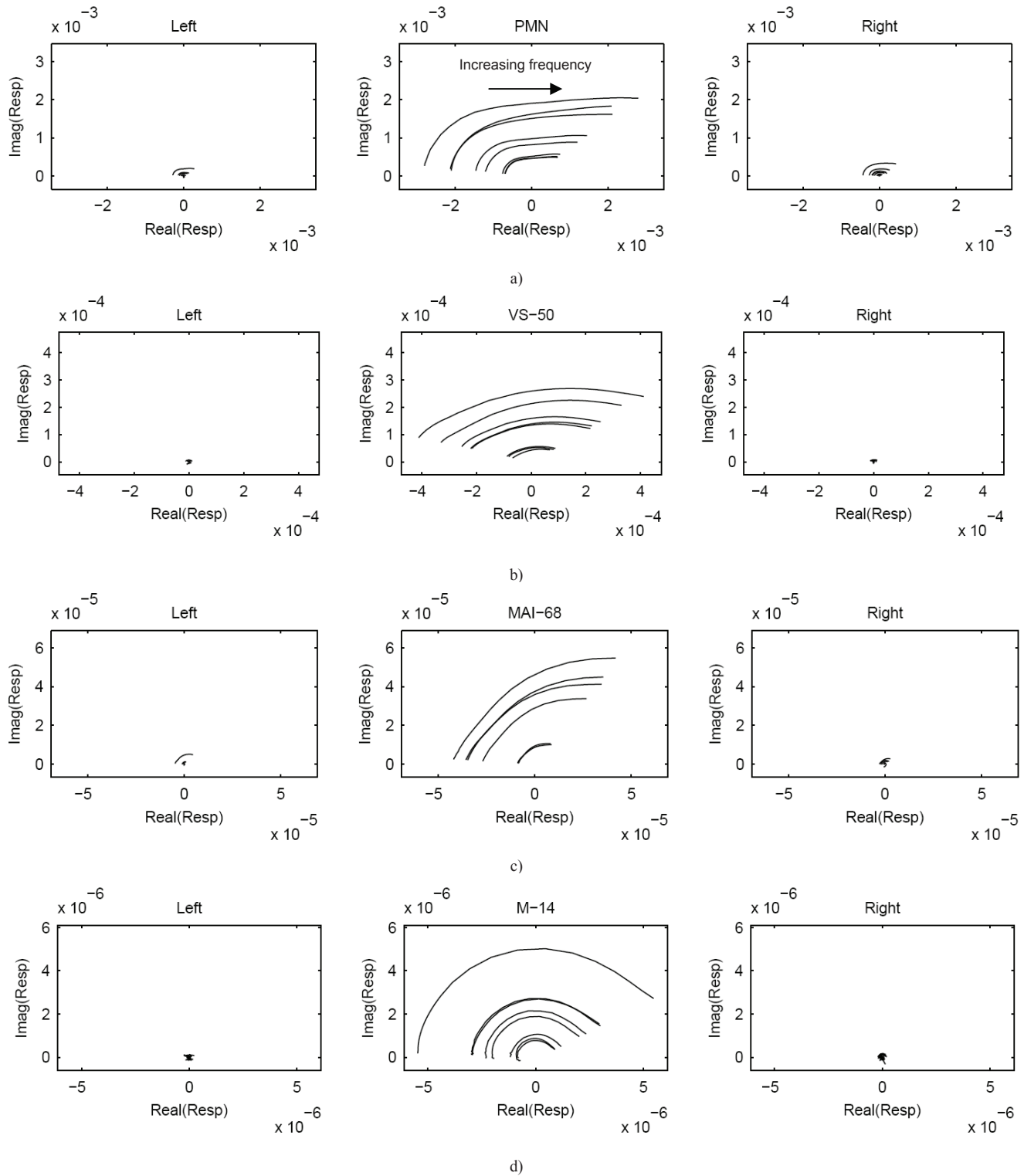


Figure 5. Response of four mines plotted on an Argand diagram for the left, center, and right receive coils when a mine is below the center of the array: a) PMN, b) VS-50, c) MAI-68, and d) M-14 anti-personnel landmines. There are 6 to 8 occurrences of each mine which are buried between 0 and 5 cm deep.